Research article

Energy harvesting from hydroelectric systems for remote sensors

Joaquim Azevedo[*] **and Jorge Lopes**

Faculty of Exact Science and Engineering, University of Madeira, Funchal, Portugal

* Correspondence: Email: jara@uma.pt; Tel: +351-291-705286.

Abstract: Hydroelectric systems are well-known for large scale power generation. However, there are virtually no studies on energy harvesting with these systems to produce tens or hundreds of milliwatts. The goal of this work was to study which design parameters from large-scale systems can be applied to small-scale systems. Two types of hydro turbines were evaluated. The first one was a Pelton turbine which is suitable for high heads and low flow rates. The second one was a propeller turbine used for low heads and high flow rates. Several turbine geometries and nozzle diameters were tested for the Pelton system. For the propeller, a three-bladed turbine was tested for different heads and draft tubes. The mechanical power provided by these turbines was measured to evaluate the range of efficiencies of these systems. A small three-phase generator was developed for coupling with the turbines in order to evaluate the generated electric power. Selected turbines were used to test battery charging with hydroelectric systems and a comparison between several efficiencies of the systems was made.

Keywords: Energy harvesting; hydroelectric power generation; experimental results; mechanical power

1. Introduction

Remote sensors require efficient power supply systems. The deployment of these sensors in areas without access to the electric grid requires energy harvesting from the environment for long-term operation [1-4]. Solar energy is currently the most used power source for energy harvesting. However, there are situations where solar sources or wind sources are not appropriate. For instance, the use of solar panels for environmental monitoring in forests has limitations due to the obstruction caused by trees. If water streams exist in those areas, small hydroelectric systems may provide enough power to supply the sensor systems for long periods.

Hydroelectric systems are extensively used for large-scale electrical power generation. For

small-scale (milliwatts to watts of power), water is usually mentioned in literature as a source of energy that may be used by harvesting systems [4-6]. However, there are virtually no studies about the performance of the hydroelectric systems at such scale. Carroll [7] proposed a patent for an energy harvesting system based on a piezoelectric membrane (5 cm high and 20 cm long) that oscillates in a water channel. The author expected to produce up to 250 mW in a flow rate of 1 m/s. This result considered an energy capture efficiency of 50%. Wang and Liu [8] developed a piezoelectric film energy harvester to generate power from pressurized water flow. The instantaneous output power was 0.45 nW for an excitation pressure of 20.8 kPa and for a frequency of 45 Hz. Lee, Sherrit et al. [9] also proposed a piezoelectric flow energy harvesting system. The harvester produced 20 mW at a flow rate of 20 L/min and for a pressure drop of 165 kPa. Using these results, the efficiency of the system was about 0.04%. A different approach was proposed by Kwon, Park et al. [10], developing a water motion transducer that converts water motion into electric energy. A power of 16.4 μW was generated with the motion of a 30 μL droplet of water. The peak power density of the system was 0.05 mW/cm^2. Morais, Matos et al. [11] used a commercial hydrogenerator designed for smart gas-based water heating as a harvesting device. The hydrogenerator was placed in irrigation pipes where a small quantity of water was derived to move the turbine coupled to a DC generator. The system produced 80 mW at a load of 100 ohm for a flow rate of 0.5 m^3/s. The work developed in [12] demonstrated the use of small turbines with a design similar to those of large scale hydroelectric systems. A Pelton turbine with a diameter of 1.6 cm produced 600 mW for a load of 90 Ω with a head of 4 m and a flow rate of 0.043×10^{-3} m^3/s. The efficiency of the system was 28%. A propeller turbine placed inside a pipe produced 350 mW for a load of 90 Ω with a flow rate of 0.6×10^{-3} m^3/s. The efficiency of this system was 5.5%. Also using a rotating machine, Hoffmann, Willmann et al. [13] developed a radial-flux energy harvester incorporating a three-phase generator for converting energy from water flow in domestic water pipelines. The energy harvester generated up to 720 mW when using a flow rate of 20 L/min with a 70 ohm load and for a pressure drop of 2.2 bar. This corresponds to a system efficiency of about 1%.

Considering the existing small-scale systems for energy harvesting from water flow, several works focused on the use of piezoelectric materials to generate electricity. Although compact, the generated power is relatively low. The efficiency of these systems is also very low. Hydroelectric turbines provide higher power levels. These systems are able to provide energy to supply remote sensors in actual environments. For instance, a wireless sensor network deployed for environmental monitoring typically uses a mesh topology. The Zigbee protocol [14] based on the 802.15.4 norm is commonly used due to its low power requirements. The typical communication radios consume a current between 10 and 40 mA when receiving and transmitting data. The power consumption is between 30 and 130 mW for a voltage of 3.3 V. Furthermore, the microcontroller, the sensors and other systems increase the energy consumption. Since a router in a wireless sensor network must be always on, the power supply system must provide tens or hundreds of milliwatts.

In this work a study on the application of hydroelectric turbines for energy harvesting is presented. The science and the technology of large-scale hydroelectric power generation are well established. The efficiencies of these systems are usually above 90%. However, the few works provided in literature which use small turbines show much lower efficiencies. Furthermore, the results vary among studies. This paper presents results for the study performed on the evaluation of two types of turbines. The first one is a propeller turbine, used for large-scale systems in situations where low heads and large flow rates are available. The second turbine is a Pelton, used for

large-scale systems in situations where high heads and low flow rates are available. The efficiencies of the systems are determined for different parameters of the hydroelectric system in order to evaluate the application of large-scale design in miniaturization.

2. Materials and Method

Several parameters of large-scale turbines may not be feasible on low power generation. For instance, the control of the orientation of the Kaplan turbine propellers is not easily scaled for small turbines. Therefore, the main parameters of design of small-scale turbines and hydroelectric systems must be determined. Round [15] stated that an efficiency improvement of 1% or 2% is worthwhile for systems generating thousands of kilowatts. This increase of efficiency may be not worthwhile in small-scale energy generation if it requires a higher complexity of the system.

2.1. Hydroelectric System Parameters

For large-scale power generation there are two main types of hydroelectric turbines depending on the height of the water column and the flow rate: impulse and reaction [16]. The impulse turbine uses the velocity of the water to move the runner. The Pelton turbine is a well-known system of this type. The reactive turbine combines the pressure and the moving water to move the runner. A well-known type is the propeller turbine.

There are several parameters used in the design and evaluation of hydroelectric machines. The power available at the turbine shaft is given by [16]

$$P = \eta_H \rho g Q H \tag{1}$$

where η_H is the hydraulic efficiency of the turbine, ρ is the density of the water (typically 1000 kg/m^3), g is the acceleration of gravity (9.8 m/s^2), Q is the flow rate (m^3/s) and H is the effective head (m). The effective head is the difference between the gross head and the head loss. The head losses are due to the frictional loss inside the tubes, the inlets loss, the losses due to bends and changes of the cross-sectional area, and so on.

The specific speed is a dimensionless parameter defined by

$$n_s = \frac{N\sqrt{P}}{\sqrt{\rho}(gH)^{\frac{5}{4}}} \tag{2}$$

with N the rotational speed (rps). A more commonly used the parameter is

$$N_s = \frac{N\sqrt{P}}{H^{\frac{5}{4}}} \tag{3}$$

This variable is dimensional and $N_s = 548.3 n_s$. Each type of turbine has a different specific speed.

The speed ratio is [15]

$$\phi = \frac{u}{\sqrt{2gH}} \tag{4}$$

with u the tip velocity. This parameter allows estimating the speed of the turbine. The rotational speed is given by

$$N = \frac{u}{\pi D} = \frac{\phi\sqrt{2gH}}{\pi D} \tag{5}$$

with D the diameter of the turbine.

The flow rate can be determined from the velocity of the fluid and from the cross-section area. For incompressible fluids the continuity equation is given by

$$Q = A_1 V_1 = A_2 V_2 \tag{6}$$

with A_1 and A_2 the transversal area of the tube at points 1 and 2, respectively, and V_1 and V_2 the velocity of water at those points. This equation indicates that the flow rate of an incompressible fluid is constant and a decrease in the area produces an increase in the velocity of the fluid.

The calculation of the effective head of the hydroelectric system requires the estimation of the head losses. For a pipe with several sections, the total head loss is given by [17]

$$h_f = \sum_{k=1}^{n} h_{fk} = \sum_{k=1}^{n} \frac{f_k L_k v_k^2}{2g D_{pk}} = \sum_{k=1}^{n} \frac{K_k v_k^2}{2g} = \sum_{k=1}^{n} \frac{8K_k Q^2}{\pi^2 g D_{pk}^4} = \beta Q^2 \tag{7}$$

with $K = fL/D_p$, where f is the friction factor (kg/ms), L is the pipe length (m), D_p is the pipe diameter (m), v is the mean velocity of the fluid and k is the section where these parameters are obtained.

2.2. Pelton Turbine

Pelton turbines are used for high heads and low flow rates. The maximum efficiency is in the range from 85% to 90% [15,17]. The typical range for the specific speed n_s is from 0.015 to 0.053 or for N_s from 8 to 29 [17]. The main parameters of the turbine are represented in Figure 1. Figure 1a shows the turbine and in Figure 1b is the bucket design. D is the diameter of the turbine and d is the diameter of the jet. The buckets have a shape of two half ellipsoids with a central splitter to allow a faster extraction of the water after transmitting its kinetic energy to the turbine. Typically, the bucket angle of attack, α, is higher than 90° (about 105°) [15].

Table 1 shows typical dimensions of design of the turbine for the best efficiency at large-scale [16,17]. It may be noted that all parameters are dependent on the jet diameter. Considering the relation D/d, the number of buckets of the turbine is about 22.

Table 1. Range of the main parameters for Pelton turbine.

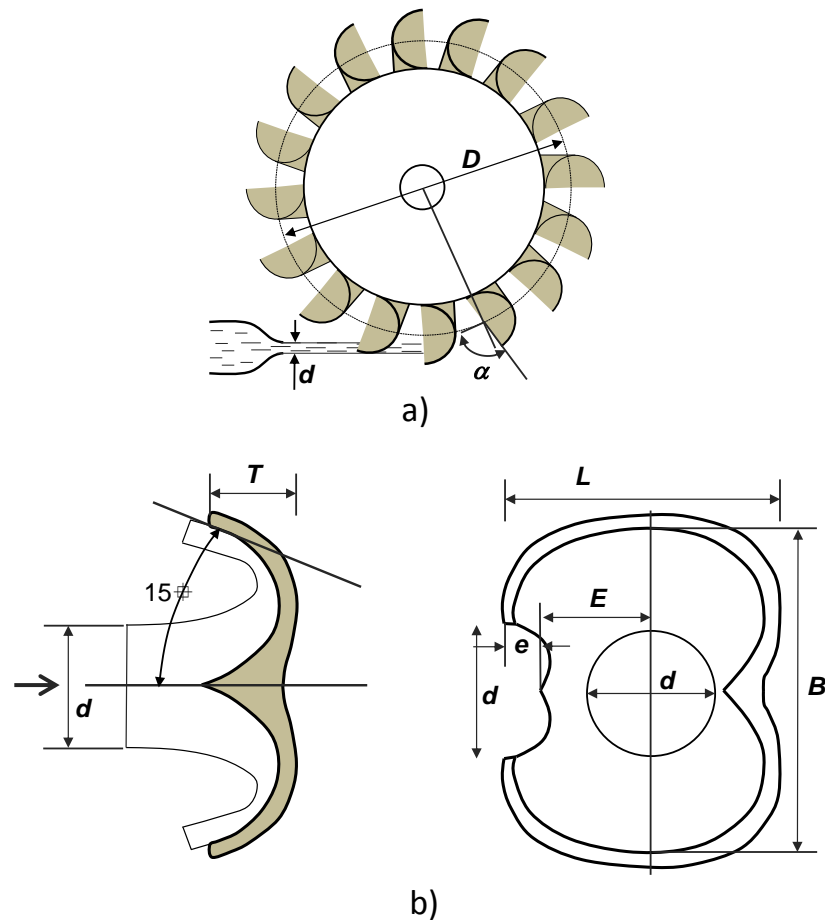| Number of buckets	D/d	B/d	L/d	T/d	e/d	E/d
$D/(2d)+15$	14–16	2.8–4	2.5–2.8	0.8–0.95	0.35	0.85

Figure 1. Pelton system: (a) turbine; (b) bucket.

The speed ratio of this turbine (ϕ) is about 0.46. The jet velocity is given by [15]

$$V_1 = C_v\sqrt{2gH} \tag{8}$$

with C_v in the range from 0.95 to 0.99. The flow rate can be calculated from

$$Q = V_1\frac{\pi d^2}{4} \tag{9}$$

Pelton turbines with small dimensions were built considering the design parameters given in Table 1. The conditions of design were: $P = 500$ mW; $\eta_H = 0.5$; $3 < H < 5$ m. From equations (1), (8), (9) and Table 1, the nozzle diameter, d, was obtained in the range from 1.6 to 2.4 mm and D in the range from 23 to 38 mm. $C_v = 0.97$ was considered in the calculation of V_1. The number of buckets obtained from Table 1 is 22 or 23. Using (5), the rotational speed, N, is in the range from 29.5 to 63 rps, giving an angular velocity (ω) in the range from 186 to 396 rad/s.

The design of the turbines follows the one of the large-scale turbine with small differences due to the very small dimensions of its details. The basic design of the turbine considered the relations: $D/d = 14$; $B/d = 4$; $L/d = 2.7$; $T/d = 0.95$; $e/d = 0.75$; $E/d = 0.9$. Nevertheless, some parameters were changed in order to determine the implications in the design of small hydrogenerators. Table 2 shows

the parameters used to produce the turbines. The number of buckets varied between 10 and 22 for a turbine with a diameter of 27 mm. To evaluate different characteristics of design each turbine differs in a specific parameter. The changes were the number of buckets, the use of a bucket angle of attack of 90° instead of 105°, the removal of the central splitter to evaluate its importance in small-scale systems and the use of a planar shape for the bucket. The turbines were created in a 3D printer.

Table 2. Dimensions of design for Pelton turbines.

Turbine	1	2	3	4	5	6	7	8	9	10	11	12	13	14
Number of buckets	10	11	12	12	15	19	22	22	22	11	11	11	11	11
D	27	27	27	27	27	27	27	27	27	31	31	31	31	31
d	2	2	2	2	2	2	2	2	2	2.2	2.2	2.2	2.2	2.2
Observations		(a)		(c)				(b)	(c)		(a)	(b)	(a)(b)	(c)

(a) Bucket angle of attack of 90°.

(b) Without central splitter.

(c) Planar bucket shape.

The nozzles were also built in a 3D printer with diameters of the output jet between 1.5 and 4 mm. Figure 2 shows the shape of the nozzle. This enables the evaluation of the system efficiency as a function of the relation D/d in order to compare with the one provided in Table 1.
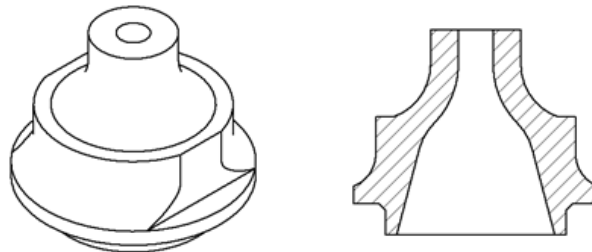

Figure 2. Nozzle configuration.

Figure 3 shows the setup for measurements and typical application. The tube connected to the injector has 18 mm of internal diameter. The nozzle is connected to the pipe that receives water from the main tank. H_m is the gross head (m). The surge tank allows to compensate the sudden variations of pressure and to remove trapped air bubbles in the vertical portion of the tube. The air purge mechanism removes air trapped near the nozzle. It consists of a system with a valve that has a floating piston that falls when there are air bubbles under it. When this happens, the valve opens enabling the purge of the air bubbles. Experiments have shown that this device is very important since the efficiency is drastically reduced due to the existence of air in the pipe. The turbine is connected to the generator that is supported in an appropriate structure. All rotating shafts are supported by ball bearings.
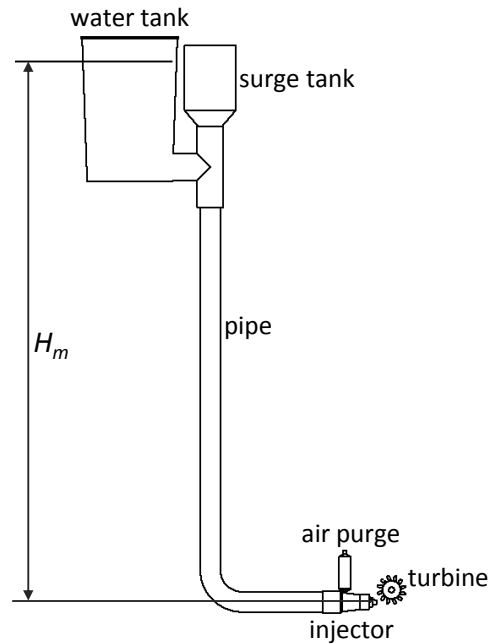
Figure 3. Experimental setup for Pelton turbine.

2.3. Propeller Turbine

Kaplan and propeller turbine Pelton turbines are used for low heads and high flow rates. The Kaplan turbine is similar to a propeller type with adjustable blade orientation. For large-scale applications, the maximum efficiency is in the range from 90% to 93% [15,16]. The typical range for the specific speed n_s is from 0.66 to 1.66 or for N_s from 362 to 910 [17]. Figure 4 shows the typical installation of the propeller turbine. The draft tube is used to reduce the loss in the head since the pressure at the outlet is below atmospheric. The diverging shape helps to convert the kinetic energy into pressure energy.
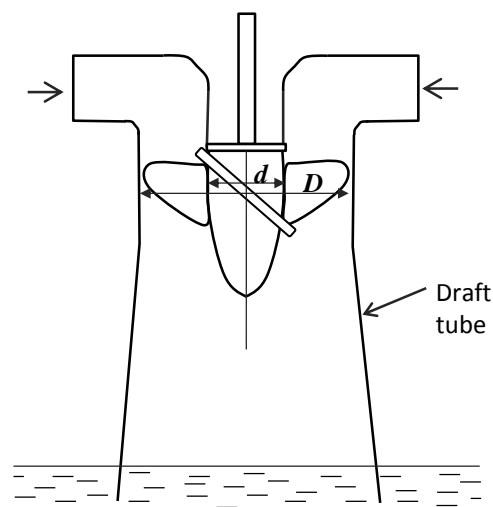

Figure 4. Propeller turbine system.

The number of blades increases with the head, being three for 5 m and 4 four for 20 m [16]. The ratio d/D is 0.3 for a head of 5 m and 0.4 for a head of 20 m. The speed ratio (ϕ) is in the rage 1.5 to 2.5. The flow rate can be determined from

$$Q = \frac{\pi}{4}(D^2 - d^2)\psi\sqrt{2gH} \tag{10}$$

with ψ in the range 0.35–0.75.

As previously mentioned, propeller turbines have 3 blades for small heads. The turbine used in this work was developed for small scale model boats (Graupner 2308.40), with the shape represented in Figure 5. It has a dimeter of 39 mm and $d = 8$ mm. The turbine was inserted in a pipe with an internal diameter of 40 mm.

Figure 5. Propeller turbine.

The conditions of design of the propeller system were: $P = 500$ mW; $\eta_H = 0.5$; $D = 39$ mm; $d = 8$ mm. From equations (1) and (10), a head of 11.7 cm is obtained. In (10) $\psi = 0.5$ was considered. For the range of speed ratios of this type of turbine, using (5) the rotational speed is in the range from 18.6 to 31 rps, giving an angular velocity in the range from 117 to 195 rad/s.

The test setup for the propeller turbine is represented in Figure 6. The turbine was mounted on a shaft with stuffing box. The shaft connects the turbine to the generator. The efficiency of divergent and non-divergent draft tubes was evaluated for different heads.
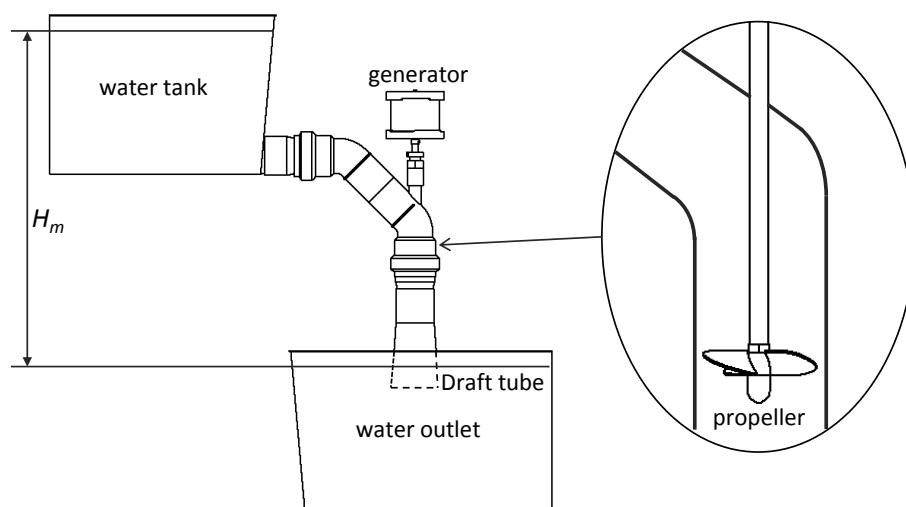

Figure 6. Experimental setup for propeller turbine.

For this system, it is important to calculate the head losses, which may be a significant fraction of the gross head. Using (7) and the *K* parameters given by Crane [18] for loss on the entrance, loss in the bends, loss at a submerged discharge, loss on a sudden expansion and loss on a sudden contraction, the total head loss is about 6 cm. For the required power mentioned previously, the gross head must be 17.7 cm. In this case, the head loss is 34% of the total head of the water column. Furthermore, the actual head loss of the developed system may be higher. For heads between 5 and 20 cm, and considering the speed ratio $\phi = 2$, the angular velocity in the range $102 < \omega < 203$ rad/s.

2.4. Hydrogenerator

For this work a three-phase permanent magnet synchronous generator was developed to convert the mechanical power into electricity. A rectifier bridge implemented with Schottky diodes and a capacitor were used to obtain direct current. The peak voltage of the generator is given by [19]

$$E_p = \frac{4qNB_pk_pr_el\omega_e}{p} = 2qNB_pk_pr_el\omega_m \tag{11}$$

where q is the number of stator coils per phase, N is the number of turns per coil, p is the number of poles, ω_e is the electrical angular velocity, ω_m is the mechanical angular velocity (rad/s), B_p is the peak air-gap flux density (T), r_e is the average radius of the stator winding (m), l is the length of the stator winding (m) and k_p is the distribution factor. The developed generator has the parameters: $q = 2$, $N = 121$; $p = 8$, $B_p = 0.087$ T; $r_e = 22$ mm, $l = 20$ mm and $k_p = 0.966$. Using $\omega_m = 200$ rad/s in (11), the peak voltage is $E_p = 3.6$ V and the rectified voltage is $V_{DC} = 3\sqrt{3}E_p/\pi = 5.9$ V, without considering the forward voltage drop across the diodes.

The generator converts the mechanical energy to electrical energy, with an efficiency defined by η_G. This is the generator and transmission system efficiencies. The rectifier converts the alternate current into a direct current with η_R of efficiency. The rectified output was connected to a programmable dynamic load to obtain the data of generated power. A system was also developed to charge batteries. In this case, a DC-DC converter was required to achieve the maximum power transfer to the load. A Cûk regulator was used since it allows to reduce the effects of electromagnetic noise due to the very low ripple of input and output current. The converter was designed to produce an output voltage of 5 V, a maximum current of 200 mA, a range for the duty cycle from 0.4 to 0.6 ($D = V_o/V_i$), 10% for the input and output current ripple and 1% for the output voltage ripple. Figure 7 shows the circuit diagram.

The Cûk regulator is typically created with two inductors, two capacitors, a diode and a controlled switch, in this case the MOSFET represented in Figure 7. The output capacitor was removed from this circuit since the battery performs the same function. The microcontroller reads the output voltage and the current and generates a PWM (Pulse Width Modulation) signal that controls the MOSFET through the driver shown in the figure. The voltage doubler allows the elevation of the voltage in order to surpass the threshold gate voltage of the MOSFET on the high terminal. The linear regulator is used to obtain the 5 V required to power supply the ATMEGA 328 microcontroller.
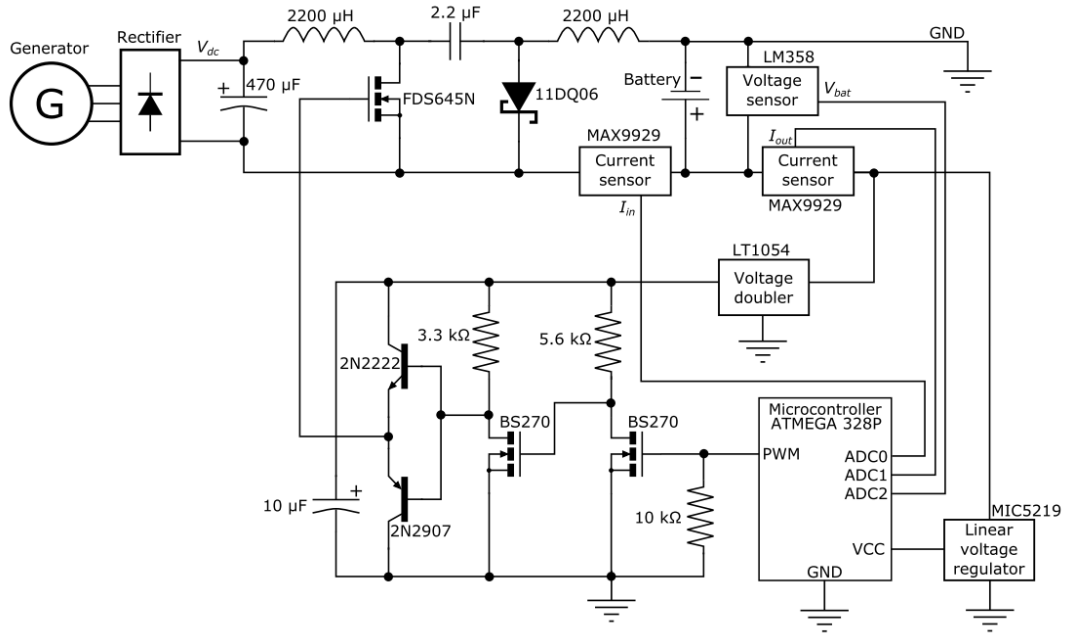
Figure 7. Block diagram of the hydroelectric system to charge batteries.

2.5. Measurement System

The efficiency of the turbines was obtained by measuring the mechanical power. The rope brake technique was used to determine the torque [20]. Figure 8 shows the system setup for torque measurements. It uses two dynamometers to measure the frictional torque introduced by a cotton thread. The hand crank allows to change the load. The cotton thread is wound around a flywheel connected to the turbine shaft.
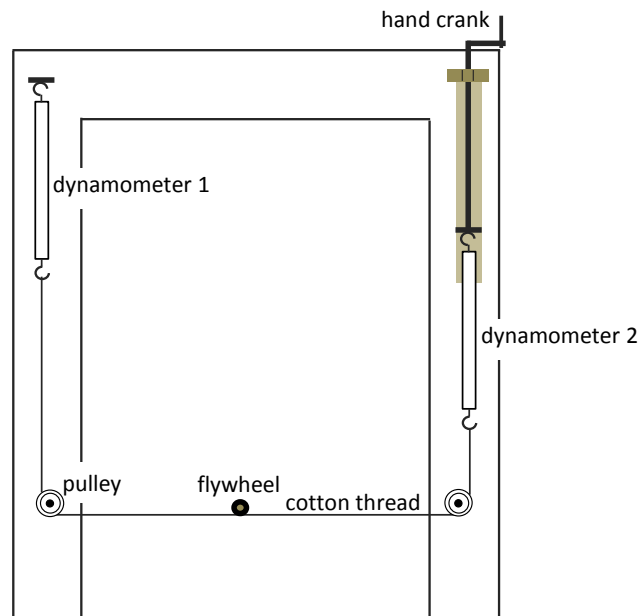

Figure 8. Scheme to measure the torque.

The torque is given by

$$\tau = (F_1 - F_2) \times r \tag{12}$$

with F_1 and F_2 the forces (N) obtained by the dynamometers (N) and r is the radius (m) of flywheel connected to the turbine under test. The flywheel has 10 mm diameter. The mechanical power is given by

$$P_m = \tau \times \omega \tag{13}$$

where ω is the angular velocity (rad/s). This velocity was measured by a hall sensor connected to a microcontroller.

3. Results and Discussion

The mechanical and electrical output powers were measured for both hydro systems. For the Pelton system the generated power was obtained for several parameters of the turbines and injectors at a fixed head. For the propeller system the generated power was evaluated as a function of the head and of the draft tube.

3.1. Mechanical Power

The mechanical power was obtained using the system shown in section 2.5. The experiments with Pelton turbines were performed for a gross head of 4.27 m. In the first column of Table 3 are the nozzle diameters used to calculate the flow rate and the effective head. The second column shows the measured flow. From (9) the jet velocity, V_1, is calculated. The effective head is obtained solving (8) in order to calculate H. As it may be observed from Table 3, the effective head is almost constant for nozzle diameters between 2.14 mm and 3.99 mm. Therefore, three different diameters within this range were used in the tests of mechanical power.

Table 3. Effective head of the Pelton system.

d (mm)	Q (m^3/s)	H (m)
1.25	0.94×10^{-5}	3.18
1.89	2.23×10^{-5}	3.52
2.14	3.05×10^{-5}	3.90
2.29	3.49×10^{-5}	3.89
2.92	5.68×10^{-5}	3.90
3.34	7.45×10^{-5}	3.92
3.99	10.56×10^{-5}	3.87
4.63	14.05×10^{-5}	3.78

Figure 9 shows the generated mechanical power for three diameters of the jet: 2.14 mm, 2.92 mm and 3.99 mm. The expected number of buckets for the turbine given by Table 1 is 22. However, the graphs demonstrate that turbines with a lower number of buckets provide better results. This can be observed from the maximum power produced by turbines 2, 3 and 5 with 11 to 15 buckets. For the same turbine, a larger nozzle dimeter (d) provides more power due to increased flow rate.
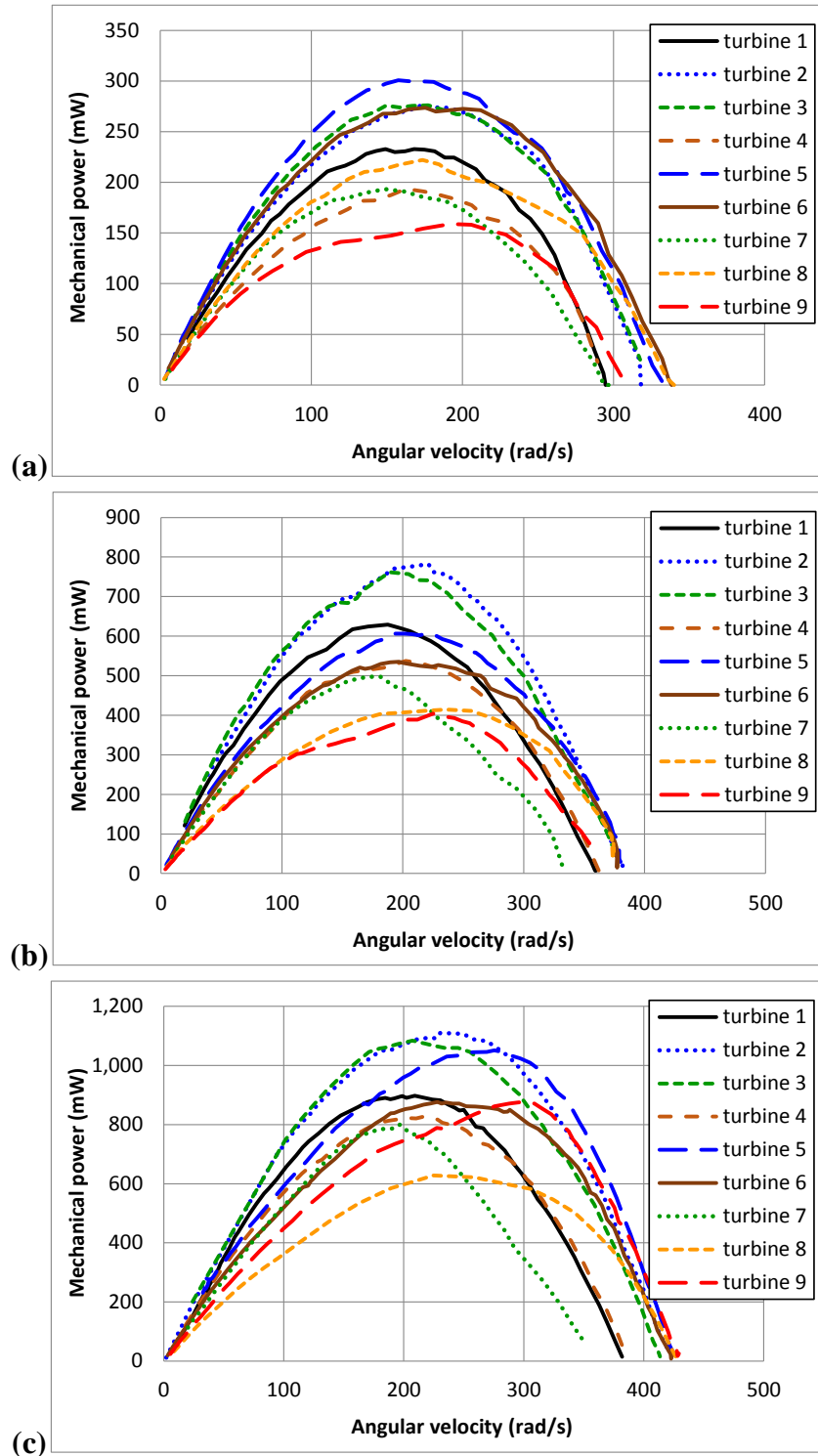
Figure 9. Mechanical power: (a) 2.14 mm; (b) 2.92 mm; (c) 3.99 mm.

The relation *D/d* is 12.6, 9.2 and 6.8 for the nozzle diameters 2.14, 2.92 and 3.99, respectively. All these values are below the range given in Table 1. From Figure 10, the higher turbine efficiencies are obtained for the nozzle diameter of 2.92 (*D/d* = 9.2). Considering the number of buckets, the best results are for turbines 2 and 3 with 11 and 12 buckets, respectively. If the number of buckets is too high the space between buckets is small, which creates difficulties in the injection of water. As

observed from Figure 10, below 11 buckets and above 15 buckets the efficiency decreases. Therefore, the relation given in Table 1 is not valid for small-scale hydroelectric systems. Turbines with planar buckets provide poor results (turbine 4 with 12 buckets and turbine 9 with 22 buckets). The central splitter of the bucket is important for the turbine design. Turbine 8 has no central splitter, producing worse results as it can be observed on graphs of Figure 9 mainly for higher nozzle diameters.

Turbines 10 to 14 have a dimeter of 31 mm and 11 buckets. They were built to test the angle of attack and the effect of the central splitter. The best result is obtained for a turbine with central splitter and an angle of attack of 90°, giving an efficiency of 39.3% (turbine 11).

Using (3) the specific speed is between 2 and 8 when the specific speeds of large-scale Pelton turbines are in the interval from 8 to 29.
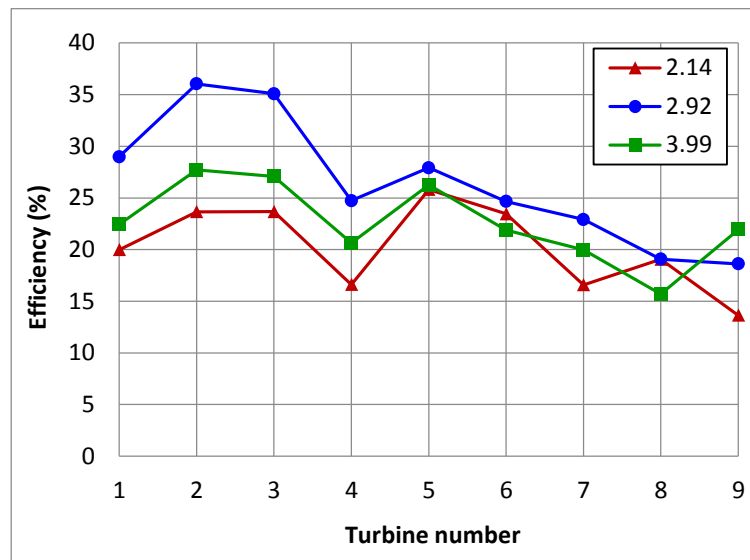

Figure 10. Efficiency for nozzle diameters of 2.14 mm, 2.92 mm and 3.99 mm.

The mechanical power of the propeller system was measured for gross heads of 10 cm, 20 cm, and 30 cm. The head loss was determined to calculate the effective head. The flow rate was measured without the turbine and the parameter β was calculated using (7). In this case, the head loss can be approximated by the gross head. Table 4 shows the parameters β obtained for several situations of the draft tube. For the gross head of 30 cm without the draft tube the water outlet is in the air. As it may be observed, β is very different from the other cases. Considering this value, the calculated head loss is higher than the gross head, meaning that the equations used to determine the effective head are not valid. Measuring the flow rate with the turbine as shown in Figure 6 and using the values of β given in Table 4, the loss head was obtained through (7). The effective heads are determined subtracting the head loss to the gross head. These values are shown in Table 4.

Table 4. Effective head of the propeller system.

Gross head (cm)	Draft tube					
	Without		Non divergent		Divergent	
	β	H (cm)	β	H (cm)	β	H (cm)
10	1.17×10^5	2.9	1.16×10^5	3.4	0.95×10^5	3.7
20	1.08×10^5	6.9	1.05×10^5	7.1	0.90×10^5	7.2
30	2.91×10^5	-	1.06×10^5	11.8	0.96×10^5	10.4

Figure 11 shows the mechanical power obtained for each mentioned situation of the propeller turbine. The divergent draft tube provided the best results for all heads. For the gross head of 30 cm without the draft tube the generated power is much lower, meaning that a discharge of water in the air results in lower efficiencies. The angular velocity for the maximum power is between 88 and 163 rad/s. For divergent draft tubes, the measured flow rate is 8.1×10^{-4}, 1.1×10^{-3} and 1.4×10^{-3} m^3/s for the heads of 3.7 cm, 7.2 cm and 10.4 cm, respectively. Using (5), the speed ratio is between 2.0 and 2.4, being inside the range given in section 2.3. Using (3), the specific speed is between 281 and 432 when the specific speeds of large-scale propeller turbines are in the interval from 362 to 910.

(a) **(b)**
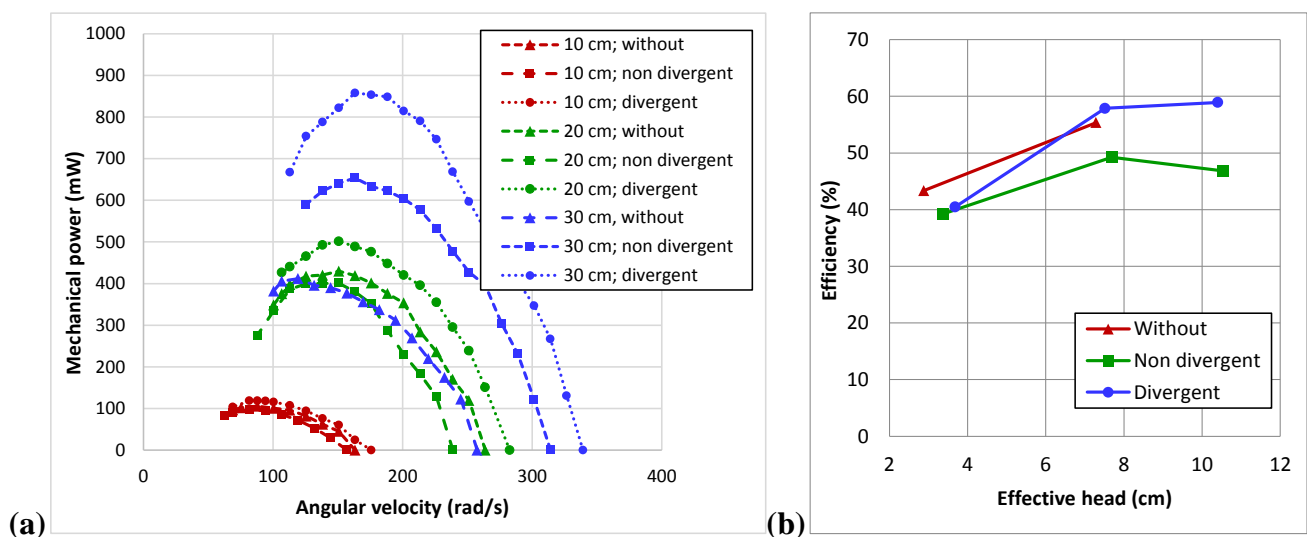
Figure 11. Mechanical power of the propeller: (a) power; (b) efficiency.

3.2. Electrical Power

The hydroelectric systems were tested for different loads in order to obtain the maximum power point. Figure 12a shows the electrical output power for the Pelton turbines. Turbine 2 ($D = 2.27$ mm) and turbine 11 ($D = 31$ mm) were evaluated for three nozzle diameters (2.29 mm, 2.92 mm and 3.99 mm). The angular velocities for the maximum power were near those of Figure 9. The loads for maximum power transfer were between 42 Ω ($d = 3.99$) and 73 Ω ($d = 2.29$) for the 27 cm diameter turbine and between 23 Ω ($d = 3.99$) and 56 Ω ($d = 2.29$) for the 31 cm diameter turbine. Figure 12b) shows the efficiencies of the turbines of Figure 12a) and also for turbine 3 (higher bucket angle of attack) and turbine 13 (without central splitter). The efficiencies are represented as a function of the output voltage to be used in maximum power transfer tracking circuits. The angle of attack did not

introduce major improvements, although with the angle of attack of 90° a better result is obtained. On the other hand, the central splitter is important to increase the efficiency as can be observed by comparing turbines 11 and 13. The efficiency of the rectifier is between 89% and 92% and the efficiency of the generator is shown in Figure 14. The efficiency of the generator increases with the rotational speed.
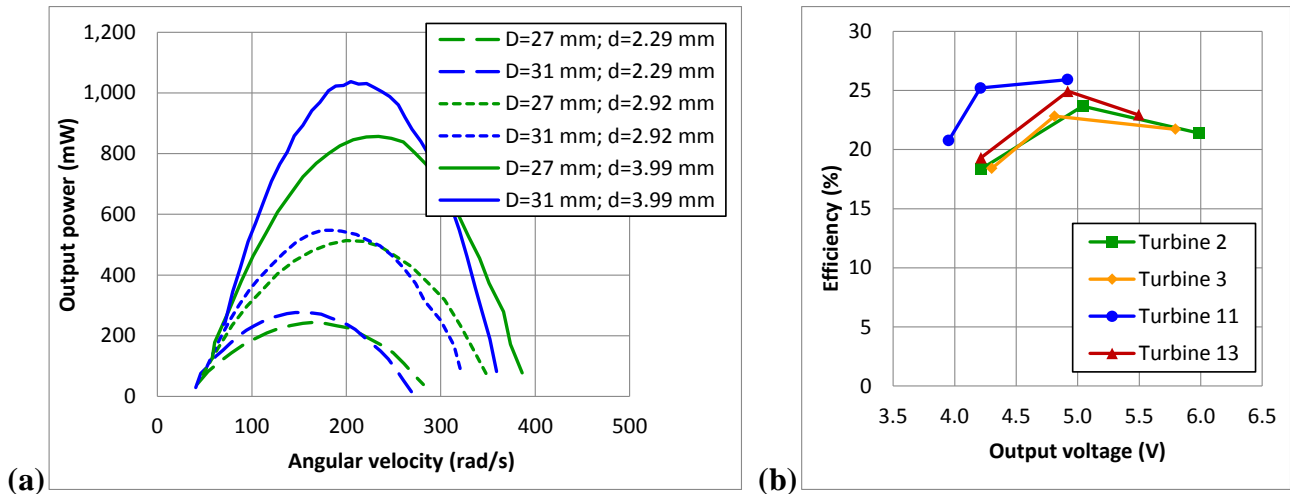

Figure 12. Pelton system: (a) output power; (b) efficiency.

Figure 13 shows the results for the propeller system for the three gross heads. The efficiencies of the rectifier are between 82% and 92% and the efficiencies of the generator are shown in Figure 14.
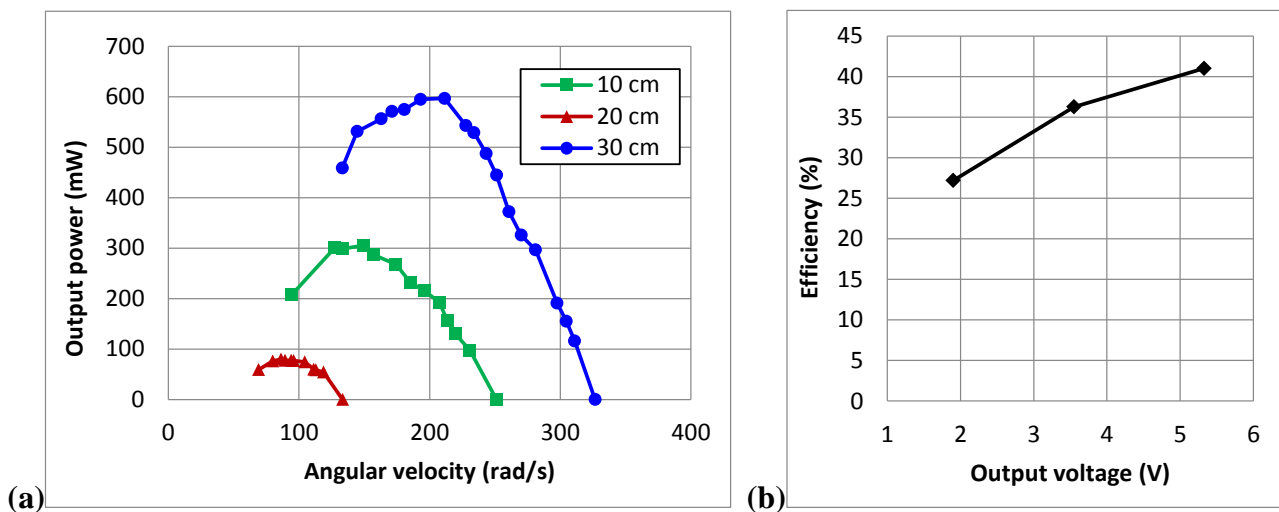

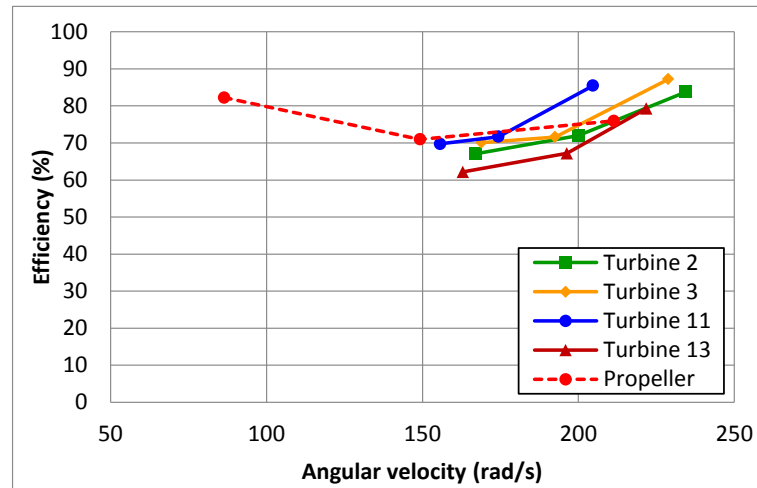**Figure 13. Propeller system: (a) output power; (b) efficiency.**

Figure 14. Efficiency of the generator.

Hydroelectric systems can be used to supply power directly to the desired loads. In contrast to several sources used in energy harvesting from the environment, hydro energy is predictable and controllable. Therefore, it may provide energy during long periods without interruption. However, hydroelectric systems may be used to charge batteries so that the mechanical lifetime of the system is extended. In this case, the system only operates during the charging period. Figure 7 shows the circuit for this purpose. The power generation of two Pelton turbines was evaluated for this operation. Figure 15 shows the results for turbine 11. Figure 15a shows the variation of the output power and the angular velocity with the duty cycle. The algorithm in the microcontroller varies this parameter for the maximum power transfer point. Figure 15b compares the output power of the DC-DC converter with the mechanical power and the electrical for maximum power transfer. The difference between the continuous and the dashed lines corresponds to the DC-DC converter efficiency. For this turbine the efficiency of the converter is 88% and the global efficiency is 22%. The efficiency of the converter for turbine 2 is 74% and the global efficiency is 17%.
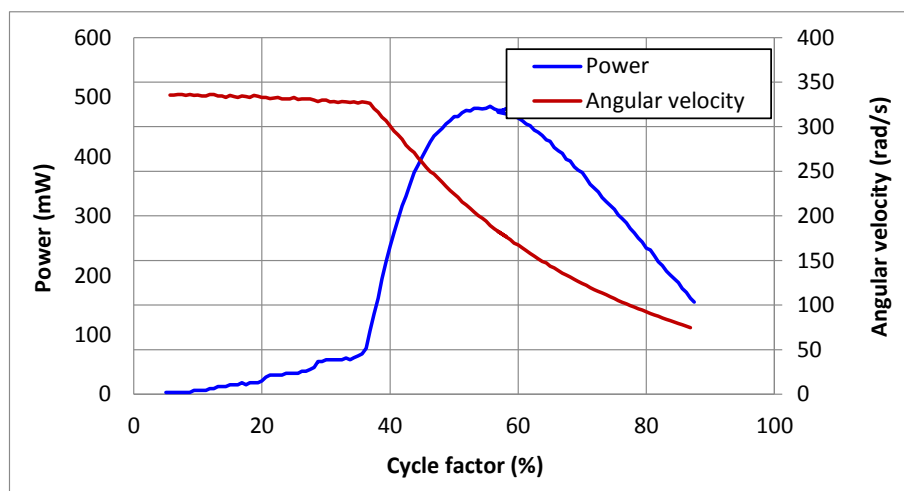

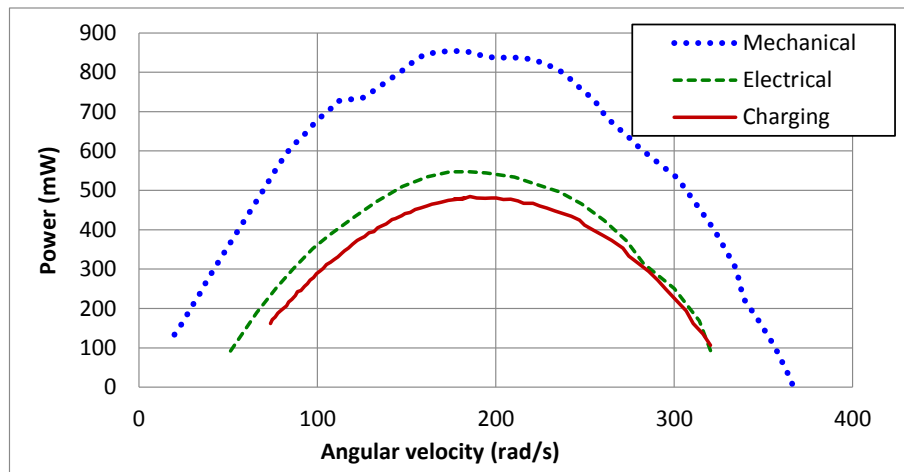**Figure 15a. Power in battery charge: output power and angular velocity as function of the duty cycle.**

Figure 15b. Power in battery charge: power comparison.

4. Conclusion

In this work a study on small-scale hydroelectric turbines was presented. Pelton and propeller turbines are appropriate to be used in energy harvesting to supply systems that consume up to hundreds of milliwatts. In applications for remote sensing with nearby water streams two typical situations may occur. The first one is when a relatively large volume of water flows through a channel. In this case, the propeller system is the most suitable for energy harvesting. The second situation is when there is a small water fall that is several meters high. In this case, the Pelton system is more appropriate for energy harvesting. Several parameters of the design of large-scale systems were evaluated for small-scale energy generation. The maximum mechanical efficiencies of Pelton turbines with diameters of 27 mm and 31 m were in the range from 35% to 40% for a head of 3.9 m. The maximum mechanical efficiencies of a propeller with a diameter of 39 mm were in the range from 57% to 59% for effective heads between 7.5 and 10.5 cm. The electrical efficiencies of the Pelton turbines were in the range from 23% to 26% and for the propeller were in the range from 36% to 41%. The number of buckets used in the design of small-scale Pelton turbine should be between 50% and 60% of the number used in large-scale. The relation between the diameters of the Pelton turbine and the jet diameter should be about 60% of that considered for large-scale. The specific speeds of both types of turbines are in the lower bounds of those for large-scale turbines. The experimental speed ratio of the Pelton turbine is slightly below the value considered for large-scale design but the speed ratio of the propeller is in the same range.

Acknowledgments

Conflict of Interest

The authors declare there is no conflict of interest.

References

1. Niyato D, Hossain E, Rashid MM, et al. (2007) Wireless sensor networks with energy harvesting technologies: a game-theoretic approach to optimal energy management. *IEEE Wireless Communication* 14: 90-96.
2. Gilbert JM, Balouchi F (2008) Comparison of energy harvesting systems for wireless sensor networks. *Int J Autom Co* 5: 334-347.
3. Wan ZG, Tan YK, Yuen C, Review on energy harvesting and energy management for sustainable wireless sensor networks. *ICCT, 2011 IEEE 13th International Conference on. IEEE*, 2011: 362-367.
4. Dewan A, Ay SU, Karim MN, et al. (2014) Alternative power sources for remote sensors: A review. *J Power Sources* 14: 129-143.
5. Thomas JP, Qidwai MA, Kellogg JC (2006) Energy scavenging for small-scale unmanned systems. *J Power Sources* 159: 1494-1509.
6. Kausar ASMZ, Reza AW, Saleh MU, et al. (2014) Energizing wireless sensor networks by energy harvesting systems: scopes, challenges and approaches. *Renew Sust Energ Rev* 38: 973-989.
7. Carroll CB (2003) Energy harvesting eel, United States Patent No.6424079.
8. Wang DA, Liu NZ (2011) A shear mode piezoelectric energy harvester based on a pressurized water flow. *Sensor Actuat A-Phys* 167: 449-458.
9. Lee HJ, Sherrit S, Tosi LP, et al. (2015) Piezoelectric Energy Harvesting in Internal Fluid Flow. *Sensors* 15: 26039-26062.
10. Kwon SH, Park J, Kim WK, et al. (2014) An effective energy harvesting method from a natural water motion active transducer. *Energ Environ Sci* 7: 3279-3283.
11. Morais R, Matos SG, Fernandes MA, et al. (2008) Sun, wind and water flow as energy supply for small stationary data acquisition platforms. *Comput Electron Agr* 64: 120-132.
12. Azevedo JAR, Santos FES (2012) Energy harvesting from wind and water for autonomous wireless sensor nodes. *IET Circ Device Syst* 6: 413-420.
13. Hoffmann D, Willmann A, Göpfert R, et al. (2013) Energy Harvesting from Fluid Flow in Water Pipelines for Smart Metering Applications. *J Phys Conf Ser* 476: 012014.
14. ZigBee Alliance. Available from: http://www.ZigBee.org.
15. Round G, Incompressible flow turbomachines: design, selection, application, and theory. Butterworth-Heinemann, 2004.
16. Murty V (2003) Hydraulic Turbines, in Logan J, Roy R, *Handbook of Turbomachinery*, New York: Marcel Dekker.
17. Kothandaraman CP, Fluid Mechanics and Machinery. New Age International, 2007.
18. Crane (1986) Flow of fluids through valves, fittings, and pipe, London: Crane Company.
19. Kamper MJ, Wang RJ, Rossouw FG (2008) Analysis and Performance of Axial Flux Permanent Magnet Machine with Air-Cored Non-overlapping Concentrated Stator Windings. *IEEE T on Ind Appl* 44: 1495-1504.
20. Singh S (2009) *Theory of Machines*, 2 Eds., Singapore: Pearson Education.